AGU PUBLICATIONS

Geophysical Research Letters

RESEARCH LETTER
10.1002/2015GL065084

Special Section:
First Results from the MAVEN Mission to Mars

Electric Mars: The first direct measurement of an upper limit for the Martian "polar wind" electric potential

Glyn Collinson[1,2], David Mitchell[3], Alex Glocer[1], Joseph Grebowsky[1], W. K. Peterson[4], Jack Connerney[1], Laila Andersson[4], Jared Espley[1], Christian Mazelle[5,6], Jean-André Sauvaud[5,6], Andrei Fedorov[5,6], Yingjuan Ma[7], Steven Bougher[8], Robert Lillis[3], Robert Ergun[4], and Bruce Jakosky[4]

[1]NASA Goddard Spaceflight Center, Greenbelt, Maryland, USA, [2]Institute for Astrophysics and Computational Sciences, Catholic University of America, Washington, District of Columbia, USA, [3]Space Sciences Laboratory, University of California, Berkeley, California, USA, [4]Laboratory For Atmospheric and Space Physics, Boulder, Colorado, USA, [5]CNRS, Institut de Recherche en Astrophysique et Planétologie, Toulouse, France, [6]University Paul Sabatier, Toulouse, France, [7]Department of Earth, Planetary, and Space Sciences, University of California, Los Angeles, California, USA, [8]Department of Atmospheric, Oceanic and Space Sciences, University of Michigan, Ann Arbor, Michigan, USA

Key Points:
- We put the first upper limit on the magnitude of the "polar wind" like parallel electric field
- The strength of this electric field is <2 V in the ionosphere
- This field is too weak to accelerate O_2^+ (the main ionospheric species) to escape velocities

Correspondence to:
G. Collinson,
glyn.a.collinson@nasa.gov

Citation:
Collinson, G., et al. (2015), Electric Mars: The first direct measurement of an upper limit for the Martian "polar wind" electric potential, *Geophys. Res. Lett.*, *42*, doi:10.1002/2015GL065084.

Received 30 JUN 2015
Accepted 20 AUG 2015

Abstract An important mechanism in the generation of polar wind outflow is the ambipolar electric potential which assists ions in overcoming gravity and is a key mechanism for Terrestrial ionospheric escape. At Mars, open field lines are not confined to the poles, and outflow of ionospheric electrons is observed far into the tail. It has thus been hypothesized that a similar electric potential may be present at Mars, contributing to global ionospheric loss. However, no direct measurements of this potential have been made. In this pilot study, we examine photoelectron spectra measured by the Solar Wind Electron Analyzer instrument on the NASA *Mars Atmosphere and Volatile EvolutioN (MAVEN)* Mars Scout to put an initial upper bound on the total potential drop in the ionosphere of Mars of $\Phi_{\sigma^{\prime}} \lessapprox \pm 2V$, with the possibility of a further $\lessapprox$4.5 V potential drop above this in the magnetotail. If the total potential drop was close to the upper limit, then strong outflows of major ionospheric species (H^+, O^+, and O_2^+) would be expected. However, if most of the potential drop is confined below the spacecraft, as expected by current theory, then such a potential would not be sufficient on its own to accelerate O_2^+ to escape velocities, but would be sufficient for lighter ions. However, any potential would contribute to atmospheric loss through the enhancement of Jeans escape.

1. Introduction

At Earth's magnetic poles, open magnetic field lines provide a pathway for ionospheric plasma to escape into the solar wind. However, in order to escape from the ionosphere, a particle must first overcome the Earth's gravitational potential. It is much harder for an ion to overcome Earth's gravity than an electron, which is 3 to 4 orders of magnitude lighter. Thus, in the absence of ions, ionospheric electrons would easily escape Earth's gravity under their own thermal pressure gradient (∇P_e). However, due to quasi-neutrality, the electrons (with density n_e, and charge e) are coupled to the ions, and an ambipolar field-aligned electric potential forms to resist their separation as in equation (1).

$$E_{||} \approx -\frac{\nabla P_e}{en_e} \tag{1}$$

Generation of this ambipolar field is critical to the formation of the classical polar wind [*Banks and Holzer*, 1968]: both retarding the outflowing electrons and reducing the effective potential barrier required for ions to escape. Superthermal photoelectrons play a particularly important role in this process [*Lemaire*, 1972], since they are much hotter (10–60 eV) [*Doering et al.*, 1976; *Peterson et al.*, 1977] than the bulk of ionospheric electrons, which have temperatures $\lessapprox$1 eV [*Pollock et al.*, 1996]. *Kitamura et al.* [2012] found the median total strength of the electric potential drop in Earth's polar wind to be $\Phi_{\oplus} = 20V$ above >3800 km.

Unlike Earth, Mars has no internal magnetic dynamo [*Smith et al.*, 1965] to stand off the solar wind, and it is the conductive Martian ionosphere in combination with localized pockets of crustal remnant field [*Acuña et al.*, 1998; *Connerney et al.*, 1999] that acts as a barrier to the interplanetary magnetic field (IMF). Magnetic field

lines pile up on the dayside, forming an "induced" magnetosphere of IMF field lines that are draped over the ionosphere. The ionosphere of Mars contains superthermal photoelectron populations, exhibiting characteristic peaks at 21–24 eV and 27 eV [*Frahm et al.*, 2006a] resulting from the photoionization of carbon dioxide and atomic oxygen. Evidence for the presence of Martian ionospheric photoelectrons was strongly suggested by data from both the *Viking* lander [*Mantas and Hanson*, 1979] and the *Mars Global Surveyor* [*Mitchell et al.*, 2001], and finally resolved by the European Space Agency *Mars Express* Analyzer for Space Plasmas and Energetic Atoms [*Barabash et al.*, 2006] Electron Spectrometer [*Lundin et al.*, 2004; *Frahm et al.*, 2006a; *Dubinin et al.*, 2006].

As in Earth's polar wind, escaping photoelectrons have been frequently observed in the Martian magnetotail. *Frahm et al.* [2006b] mapped photoelectrons throughout the tail, to the highest altitudes (3 Mars radii) explored by the *Mars Express*, and a follow up study, *Frahm et al.* [2010] calculated the mean flux of escaping photoelectrons to be $\sim 4 \times 10^6$ cm$^{-2}s^{-1}$. It has thus been hypothesized [*Dubinin et al.*, 2011] that, as at Earth, these hot photoelectrons may also generate a polar-wind-like ambipolar electric field at Mars, contributing extensively to atmospheric loss. Such a process would be global (with the exception of the Martian crustal anomalies), due to the fact that most ionospheric magnetic field lines are open, whereas at Earth the polar wind is confined only to the open field lines at the polar caps. However, in this study, we have opted to retain the nomenclature of the "polar wind" for clarity, since we investigate the same fundamental mechanism, although "electric wind" might perhaps be a more appropriate scientific description for this process.

In this pilot study, we use field-aligned electron measurements by the Solar Wind Electron Analyzer (SWEA) aboard the new NASA *Mars Atmosphere and Volatile EvolutioN (MAVEN)* Mars Scout [*Jakosky et al.*, 2015] to put the first upper bound on the strength of the Martian ambipolar polar-wind-like electric field and investigate the presence of Coloumb collisional backscattering of these electrons, which at Earth is an important source of topside ionospheric heating.

2. Method

Although very important to terrestrial atmospheric loss, the polar wind ambipolar electric field is relatively weak, with a total potential drop of perhaps only ≈20 V [*Kitamura et al.*, 2012]. Measuring such a weak field directly is thus very challenging, even with long wire booms such as those on *CLUSTER* or the *Magnetospheric Multiscale* Mission, and no such instruments are available at Mars. In this study, we use two techniques to probe parallel electric fields above and below the spacecraft, both of which require the spacecraft to be located on an open field line and above the photoelectron production region (at Mars peaking at 150 km [*Bougher et al.*, 2015]).

Figure 1 illustrates these techniques showing how three hypothetical scenarios (each with different strengths and vertical structure of the potential, viz., above or below the spacecraft) would manifest in field-aligned electron spectra. As with our later results, electrons measured outflowing tailward from the ionospheric source region are shown in blue, and the returning electrons, inflowing sunward back into the planet are shown in red. For simplicity, in these sketches the only source of electrons is assumed to be the ionosphere. The blue ionospheric spectra (identical in every panel) is based on actual *MAVEN* SWEA data and clearly exhibits the three canonical features of photoelectrons, namely, (1) the CO_2 photopeak at 23 eV; (2) an abrupt cutoff at ≈75 eV due to a sharp drop in the intensity of the solar irradiance below 16 nm [*Gan et al.*, 1990; *Richards and Peterson*, 2008], referred to as the "Aluminum (Al) Edge"; and (3) a peak of Oxygen Auger electrons at ∼500 eV.

Figure 1a shows the baseline case for a very weak electric field below the detection threshold of the instrument, both above and below the spacecraft. In this case, the only electrons observed returning to the planet are the fraction that have been backscattered through Coulomb collisions or waves. (Note that the scattering shown in Figure 1 is highly simplistic, since in reality the fraction that is backscattered is a function of energy).

Figure 1b shows the case for an Earth-like 20 V ambipolar potential above the spacecraft. In this case the downflowing spectra exhibits a discontinuity at 20 eV. Below, the entire photoelectron population is electrostatically mirrored back toward the ionosphere by the electric field and is observed at the same flux as the outgoing population. Above 20 eV, the only electrons observed returning to the planet are the fraction that has been backscattered. This scenario reflects the case at Earth, as reported by *Kitamura et al.* [2012] who found that whilst there is a great deal of variability in the terrestrial ambipolar field, the median value is 20 V

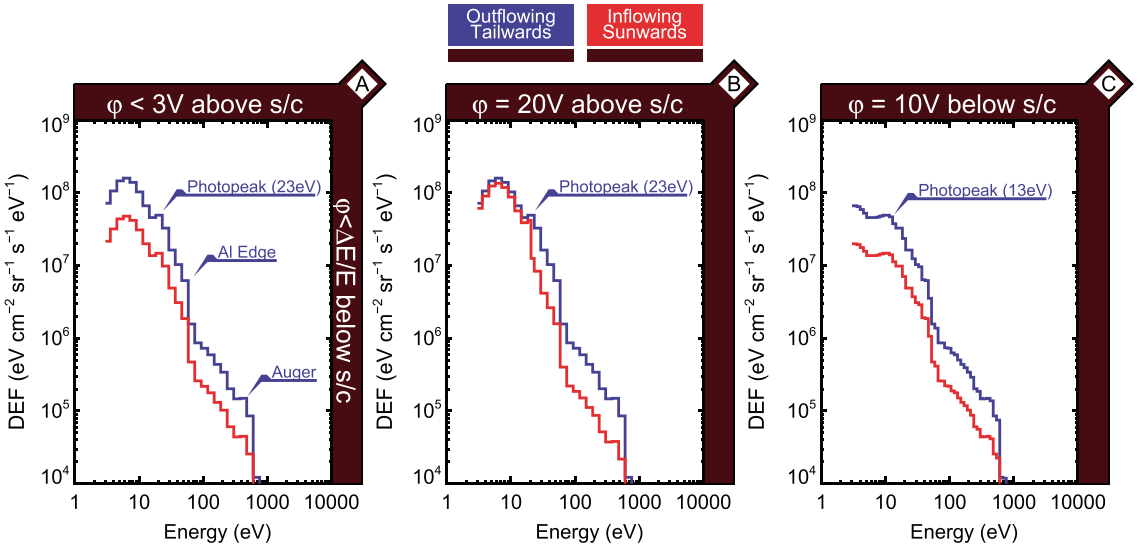

Figure 1. Sketches showing the predicted spectra of photoelectrons in the tail of Mars in the cases of (a–c) three hypothetical combinations of ambipolar field strengths. The upward spectra are shown in red and sketched downward spectra in blue.

above an altitude of ~3800 km. Our ability to measure electric potential above the spacecraft is thus limited by the lowest energy which our instrument can measure, which for SWEA is 3 eV.

Figure 1c shows another scenario, a 10 V potential drop below the spacecraft. In this case, the electric field acts to retard electrons coming off of the planet, and the entire distribution becomes shifted to lower energies. Thus, as long as the spacecraft potential is taken into account, then the electric potential below the spacecraft may be measured through any shifts in spectral features. Such a technique was recently applied by *Coates et al.* [2015], who put an upper limit of <2.95 V for the polar wind ambipolar field at Titan. The limiting factor in this technique is thus the ability of the instrument to resolve shifts in spectral features. Given the 17% energy resolution ($\Delta E/E$) of SWEA, this corresponds to ±2 eV resolution of the 23 eV photopeak, and a corresponding ±2 V upper limit on the electric potential.

3. Results: Comparing Outflowing and Inflowing Photoelectron Spectra at Mars

Figure 2 shows a map of orbit № 867, occurring on 12 March 2015. This orbit was chosen so that as the *MAVEN* flew down the magnetotail, her flight path held close to a radius ≈1 R_M from the Mars-Sun line. This course kept her on open field lines connected to the dayside, and precisely where *Frahm et al.* [2006a] mapped significant photoelectron escape, and thus ideally placed the *MAVEN* in the region of space where a Martian polar wind has been predicted. The light blue line running parallel to the orbital path shows the region from which *MAVEN* data are shown in Figure 3. Altitude (Figure 3a) and three-component magnetometer measurements (Figure 3b) are shown for reference and context. Figure 3c shows an electron spectrogram from SWEA, with time on the *x* axis (with the same range as Figures 3a and 3b), energy in eV on the *y* axis, and color denoting the $\log_{10}$ of differential energy flux in eV cm^{-2}sr^{-1}s^{-1}eV^{-1}.

Shown beneath are three electron spectra which have been ordered by the magnetic field vector. Each spectra (α, β, and γ) shows two distributions: one a field-aligned spectra (summed within ±45° of $\hat{\mathbf{B}}$) and the other an antialigned spectra (summed within ±45° of $-\hat{\mathbf{B}}$). The two spectra have been colored so that consistent with Figure 1, blue denotes the distribution of tailward flowing electrons (away from the planet), and red the sunward flowing distribution (toward the planet). Three spectra are shown from three regions: Scan alpha ("α," Figure 1, left), a pure photoelectron distribution measured near periapsis in the dayside ionosphere; Scan gamma ("γ," Figure 1, right), was measured in the wake of Mars exhibiting a hot tail of shocked solar wind electrons, indicating connection to the solar wind on both ends of the field line; Finally, scan beta ("β," Figure 1, middle) measured at an altitude of 827 km represents our current best example of a spectra taken in the right place and at the right time, to search for traces of a field-aligned "polar wind" electric potential.

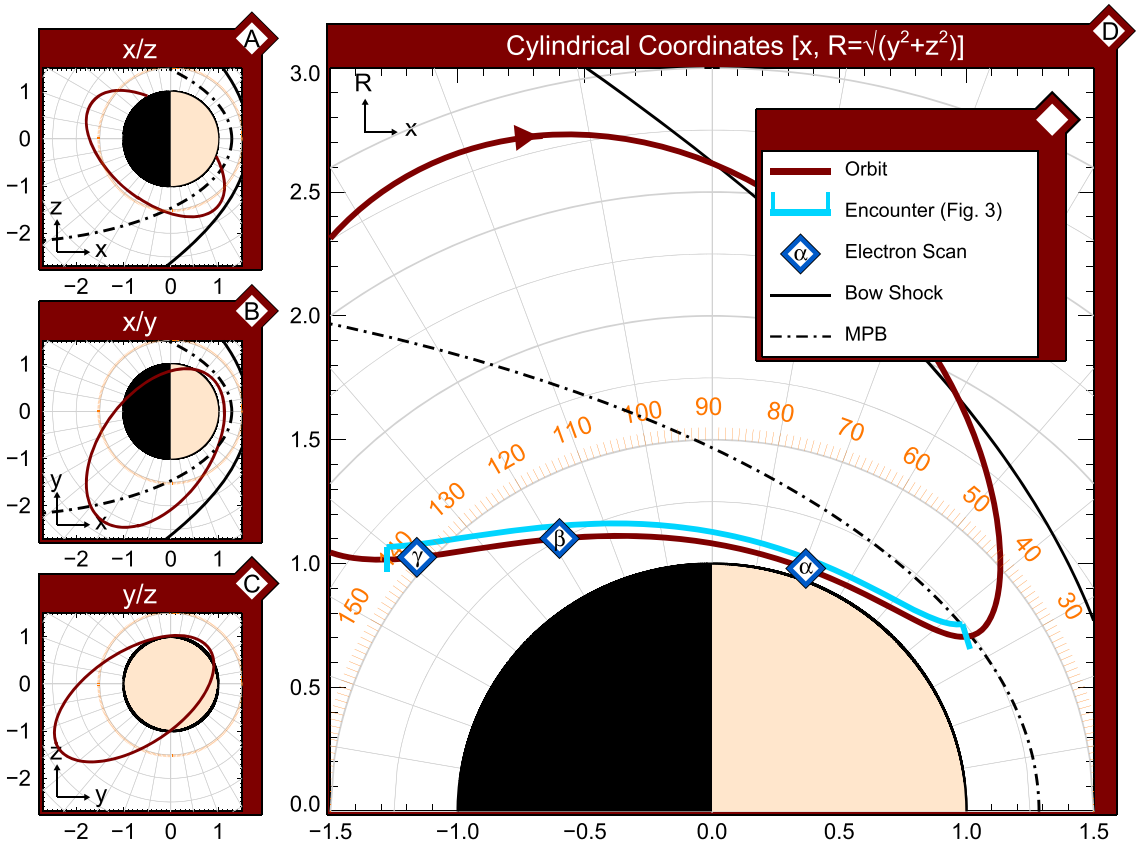

Figure 2. Map of *MAVEN* orbit № 867. The coordinate system is Mars Solar Orbital, where *x* points toward the Sun, *y* points backward along the tangent of the planetary orbit, and *z* completes the right-handed set pointing up out of the plane of the ecliptic out of the northern hemisphere. The orbit of the *MAVEN* Mars Scout is shown in red, with a model bow shock and magnetic pileup boundary (ionopause) in black, according to *Vignes et al.* [2000].

When comparing outflowing (blue) and inflowing (red) spectra in scan β, we observe two features that show that the *MAVEN* was ideally placed to observe the predicted polar wind potential: First, given that the outflowing electron population is a canonical photoelectron spectra (α), with photopeak and aluminum edge, *MAVEN* was on a field line connected to the dayside ionosphere, consistent to the outflow described by *Frahm et al.* [2006a, 2010]. Second, from the hot tail of shocked solar wind electrons inflowing, we are on an open field line also connected to the solar wind. Although only one example is shown, electron scan "β" is representative of what was uniformly observed above the source region and on open field lines (~200 km and above).

Potential drop in the Martian ionosphere. With the exception of the presence of the inflowing solar wind electrons, electron scan β most closely resembles the scenario shown in Figure 1a. The photoelectron peak is at the expected energy and any shifts resulting from an electric field below the spacecraft, if present, are too subtle to be resolved by our instrument. At 23 eV, the 17% energy resolution corresponds to a resolution of ±2 eV. Any field below the spacecraft must therefore be weaker than ±2 V. Thus, as with *Coates et al.* [2015] at Titan, we observe no evidence for a polar wind ambipolar potential drop in the topside ionosphere of Mars, and if present, it is so weak that it cannot be resolved.

An important consideration when applying this technique is correcting for the spacecraft potential. Using the Langmuir Probe and Waves experiment aboard *MAVEN*, we independently measured this potential to be −1.5 V ± 0.5 V during scan "β." Thus, any effects due to the spacecraft potential would have also been smaller than the resolution of SWEA and does not affect our conclusion that we do not observe any evidence for a shift in photoelectron spectra, and thus any electric fields in the topside ionosphere of Mars must be weaker than 2 V.

Total potential drop in the Martian magnetotail. When we compare the spectra at lower energies (<75 eV), we find that the inflowing spectra is at a lower flux than the outflowing population, but maintaining the same shape characteristic of photoelectrons. Since there is no source of photoelectrons in the solar wind, the

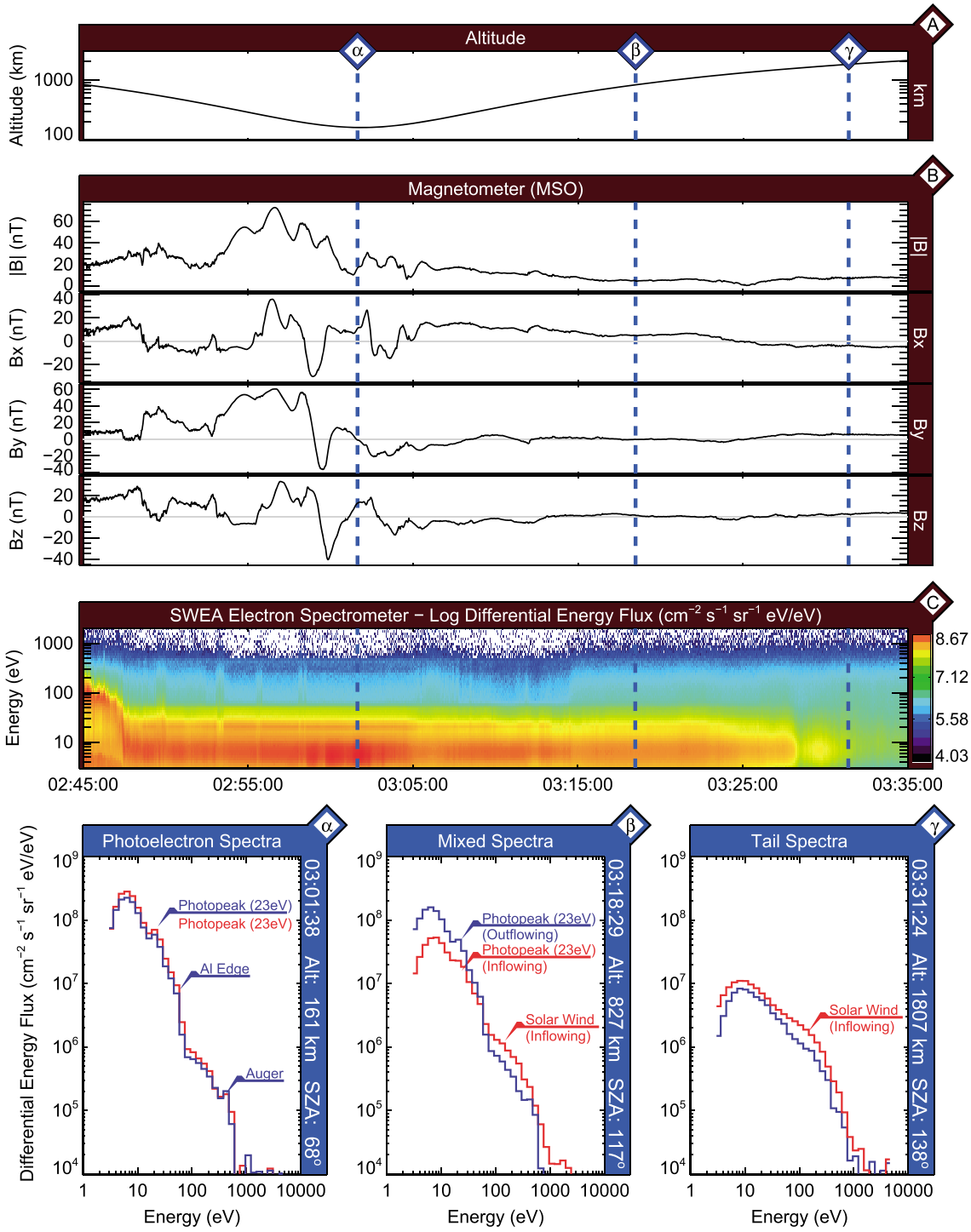

Figure 3. Magnetic and electron observations from the NASA *MAVEN* Mars Scout on orbit № 867.

presence of a photopeak in the inflowing spectra is indicative that the downflowing population in this energy range is a result of backscattering from either Coloumb collisions or waves. We find no evidence for a discontinuity below which the fluxes were equal, as would be expected in the presence of an ambipolar electric field above the spacecraft [*Kitamura et al.*, 2012]. Thus, we conclude that if there is an electric potential in the magnetotail, it is too weak to be measured by SWEA. We therefore put an upper limit on the potential drop in the magnetotail of 4.5 V, resulting from a combination of the lower limit of the SWEA sensor (<3 V) and the spacecraft potential (1.5 V).

4. Discussion

The spectral signature of inflowing electrons in Figure 3, spectra β, are most consistent with what would be expected if electron scattering was the sole process occurring (Figure 1a). Surprisingly, the photoelectron driven parallel electric field, predicted by *Frahm et al.* [2010] and *Dubinin et al.* [2011], are not identified in this first observation. These data allow us to put the first upper bounds on the ambipolar electric field potential drop in the ionosphere of Mars of $\Phi_{\sigma^{\prime}} \lessapprox \pm 2V$. Whilst there is the possibility of an additional < 4.5 V potential drop above in the magnetotail, current theory would suggest that this is less likely, given that $E_{||}$ is driven by ∇P_e and based on *Viking* observations by *Hanson et al.* [1977]; we expect the majority of the electron pressure gradient to be below 350 km.

Thus, despite a gravitational field one third of Earth's, the polar wind ambipolar electric potential measured at Mars on *MAVEN* orbit № 867 was at least a factor of 3 weaker than at Earth, if not more. The energy required for ionospheric escape is 0.1 eV for H^+, 2.1 eV for O^+, and 4.2 eV for O_2^+. If the total potential drop (above and below *MAVEN*) were close to the upper limit of 6.5 V, then the potential would be more than sufficient to allow all species to escape. However, if as current theory suggests that most of the potential drop is located below the spacecraft in the ionosphere, then a potential drop on the order of ± 2 V would have disparate effects depending on species. It would be too weak to impart enough energy for O_2^+, the main species in the lower ionosphere to escape. However, it would be just sufficient for O^+ and more than sufficient for H^+. Measurements by Viking demonstrate that these later species become dominant in the upper ionosphere [*Hanson et al.*, 1977]. O_2^+ is expected to drop off faster than these lighter ions due to scale height effects in a hydrostatic atmosphere. However, transport effects become more important at higher altitudes and an electric potential may be a contributing factor in further separating these species.

If typical, then the electric potential at Mars is more comparable with unmagnetized Titan than magnetized Earth and would have implications for the relative importance of the polar wind mechanism on atmospheric escape and evolution at Mars. However, it is important to note that any electric potential (however slight) would still reduce the potential barrier and enhance Jeans escape [*Moore and Khazanov*, 2010].

One possible explanation for such a weak ambipolar electric field at Mars is that, unlike the Earth's magnetotail, the wake is filled with penetrating hot shocked solar wind electrons (e.g., Figure 3, spectra β, γ). The presence of these superthermal electrons may serve to counterbalance the photoelectrons in satisfying the quasi-neutrality and currentless conditions, thereby reducing the parallel electric field required. To test this hypothesis we compare the relative fluxes of incoming solar wind to outgoing planetary electrons. As a first approximation we divide the spectra into two energy ranges: photoelectron dominated (below 60 eV) and solar wind dominated (above 60 eV). We then integrate spectrum β over each range in order to determine the net number flux. The net inflowing solar wind number flux is approximately one third of the outgoing photoelectron flux. This differs from the majority of Earth's polar regions (apart from the cusp), where the solar wind does not have direct entry.

5. Conclusions

The presence of a field-aligned "polar wind" like electric potential has been hypothesized to exist in the magnetotail of Mars based on the frequent observation of outflowing superthermal photoelectrons [*Frahm et al.*, 2006a, 2010]. Thus, it is assumed that this field may play an important role in the atmospheric loss at these planets [*Dubinin et al.*, 2011]. However, such an electric field has never been directly observed.

On 12 March 2015, the orbit of the *MAVEN* Mars Scout was ideally placed to fly down the corridor where this field has been predicted. We examined known spectral features in the outflowing population of photoelectrons, finding no evidence for any appreciable shift expected from an electric potential drop below the spacecraft. This technique is limited by the 17% energy resolution of SWEA, which at 23 eV corresponds to ± 2 eV. We thus place an upper limit on the polar wind electric potential drop in the ionosphere of $\Phi_{\sigma^{\prime}} \lessapprox \pm 2V$. Additionally, we compared the relative fluxes between these populations to determine the total field-aligned electric potential drop above the *MAVEN* in the magnetotail, finding an upper limit of 4.5 V. However, given that this field is driven by the electron pressure gradient and the majority of the gradient is in the ionosphere, we would therefore expect the majority of $E_{||}$ to be spatially located in the ionosphere. Thus, we find the polar wind potential to be weaker than the median value at Earth ($\Phi_{\pm_{\oplus}} = 20V$ [*Kitamura et al.*, 2012]) and may not be sufficient to directly accelerate an O_2^+ ion (the primary constituent of the lower ionosphere) to escape velocity

but may be sufficient for lighter ion species. However, any electric field would still contribute to atmospheric loss through reducing the potential barrier, thus enhancing Jeans escape [*Moore and Khazanov*, 2010].

We also find significant evidence for scattering in the Martian tail (along the field line above the spacecraft). At Earth, such scattering creates the topside electron heat flux and plays a significant role in controlling the scale height of the topside ionosphere. Further observations and modeling are required to (a) determine whether these electric potentials are typical and (b) whether collisions are sufficient to generate the topside electron heat flux on their own.

Acknowledgments
MAVEN data are available from the NASA Planetary Data System. This work was partially supported by the CNES for the part based on observations with the SWEA instrument embarked on *MAVEN*.

The Editor thanks an anonymous reviewer for assisting in the evaluation of this paper.

References

Acuña, M. H., et al. (1998), Magnetic field and plasma observations at Mars: Initial results of the Mars global surveyor mission, *Science*, *279*, 1676–1680, doi:10.1126/science.279.5357.1676.

Banks, P. M., and T. E. Holzer (1968), The polar wind, *J. Geophys. Res.*, *73*, 6846–6854, doi:10.1029/JA073i021p06846.

Barabash, S., et al. (2006), The Analyzer of Space Plasmas and Energetic Atoms (ASPERA-3) for the Mars express mission, *Space Sci. Rev.*, *126*, 113–164.

Bougher, S. W., D. A. Brain, L. J. Fox, F. Gonzalez-Galindo, C. Simon-Wedlund, and P. G. Withers (2015), Chapter 14: Upper Atmosphere and Ionosphere, in *Mars Book II*, edited by B. Haberle et al., Cambridge Univ. Press, in press.

Coates, A. J., A. Wellbrock, J. H. Waite, and G. H. Jones (2015), A new upper limit to the field-aligned potential near titan, *Geophys. Res. Lett.*, *42*, 4676–4684, doi:10.1002/2015GL064474.

Connerney, J. E. P., M. H. Acuña, P. J. Wasilewski, N. F. Ness, H. Rème, C. Mazelle, D. Vignes, R. P. Lin, D. L. Mitchell, and P. A. Cloutier (1999), Magnetic lineations in the ancient crust of Mars, *Science*, *284*, 794–798, doi:10.1126/science.284.5415.794.

Doering, J. P., W. K. Peterson, C. O. Bostrom, and T. A. Potemra (1976), High resolution daytime photoelectron energy spectra from AE-E, *Geophys. Res. Lett.*, *3*, 129–131, doi:10.1029/GL003i003p00129.

Dubinin, E., M. Fränz, J. Woch, E. Roussos, S. Barabash, R. Lundin, J. D. Winningham, R. A. Frahm, and M. Acuña (2006), Plasma morphology at Mars. Aspera-3 observations, *Space Sci. Rev.*, *126*, 209–238, doi:10.1007/s11214-006-9039-4.

Dubinin, E., M. Fraenz, A. Fedorov, R. Lundin, N. Edberg, F. Duru, and O. Vaisberg (2011), Ion energization and escape on Mars and Venus, *Space Sci. Rev.*, *162*, 173–211, doi:10.1007/s11214-011-9831-7.

Frahm, R. A., et al. (2006a), Carbon dioxide photoelectron energy peaks at Mars, *Icarus*, *182*, 371–382, doi:10.1016/j.icarus.2006.01.014.

Frahm, R. A., et al. (2006b), Locations of atmospheric photoelectron energy peaks within the Mars environment, *Space Sci. Rev.*, *126*, 389–402, doi:10.1007/s11214-006-9119-5.

Frahm, R. A., et al. (2010), Estimation of the escape of photoelectrons from Mars in 2004 liberated by the ionization of carbon dioxide and atomic oxygen, *Icarus*, *206*, 50–63, doi:10.1016/j.icarus.2009.03.024.

Gan, L., T. E. Cravens, and M. Horanyi (1990), Electrons in the ionopause boundary layer of Venus, *J. Geophys. Res.*, *95*, 19,023–19,035, doi:10.1029/JA095iA11p19023.

Hanson, W., S. Sanatani, and D. Zuccaro (1977), The Martian ionosphere as observed by the Viking retarding potential analyzers, *J. Geophys. Res.*, *82*(28), 4351–4363.

Jakosky, B., et al. (2015), The Mars Atmosphere and Volatile EvolutioN *(MAVEN)* mission, *Space Sci. Rev.*, 1–46, doi:10.1007/s11214-015-0139-x.

Kitamura, N., K. Seki, Y. Nishimura, N. Terada, T. Ono, T. Hori, and R. J. Strangeway (2012), Photoelectron flows in the polar wind during geomagnetically quiet periods, *J. Geophys. Res.*, *117*, A07214, doi:10.1029/2011JA017459.

Lemaire, J. (1972), Effect of escaping photoelectrons in a polar exospheric model, *Space Res.*, *12*, 1413–1416.

Lundin, R., et al. (2004), Solar wind-induced atmospheric erosion at Mars: First results from ASPERA-3 on Mars express, *Science*, *305*, 1933–1936.

Mantas, G. P., and W. B. Hanson (1979), Photoelectron fluxes in the Martian ionosphere, *J. Geophys. Res.*, *84*, 369–385, doi:10.1029/JA084iA02p00369.

Mitchell, D. L., R. P. Lin, C. Mazelle, H. Rème, P. A. Cloutier, J. E. P. Connerney, M. H. Acuña, and N. F. Ness (2001), Probing Mars' crustal magnetic field and ionosphere with the MGS electron reflectometer, *J. Geophys. Res.*, *106*, 23,419–23,428, doi:10.1029/2000JE001435.

Moore, T. E., and G. V. Khazanov (2010), Mechanisms of ionospheric mass escape, *J. Geophys. Res.*, *115*, A00J13, doi:10.1029/2009JA014905.

Peterson, W. K., J. P. Doering, T. A. Potemra, R. W. McEntire, and C. O. Bostrom (1977), Conjugate photoelectron fluxes observed on atmosphere explorer C, *Geophys. Res. Lett.*, *4*, 109–112, doi:10.1029/GL004i003p00109.

Pollock, C. J., T. E. Moore, M. L. Adrian, P. M. Kintner, and R. L. Arnoldy (1996), SCIFER-Cleft region thermal electron distribution functions, *Geophys. Res. Lett.*, *23*, 1881–1884, doi:10.1029/96GL01486.

Richards, P. G., and W. K. Peterson (2008), Measured and modeled backscatter of ionospheric photoelectron fluxes, *J. Geophys. Res.*, *113*, A08321, doi:10.1029/2008JA013092.

Smith, E. J., L. Davis, P. J. Coleman, and D. E. Jones (1965), Magnetic field measurements near Mars, *Science*, *149*(3689), 1241–1242.

Vignes, D., C. Mazelle, H. Rme, M. H. Acuña, J. E. P. Connerney, R. P. Lin, D. L. Mitchell, P. Cloutier, D. H. Crider, and N. F. Ness (2000), The solar wind interaction with Mars: Locations and shapes of the bow shock and the magnetic pile-up boundary from the observations of the MAG/ER Experiment onboard Mars Global Surveyor, *Geophys. Res. Lett.*, *27*, 49–52, doi:10.1029/1999GL010703.